

# Ring-Fused Diphenylchlorins as Potent Photosensitizers for Photodynamic Therapy Applications: In Vitro Tumor Cell Biology and in Vivo Chick Embryo Chorioallantoic Membrane Studies

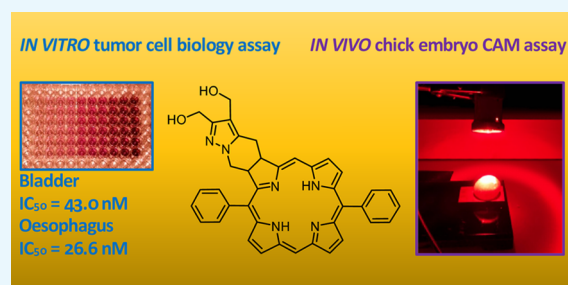
Bruno F. O. Nascimento,<sup>†</sup> Mafalda Laranjo,<sup>‡,⊥</sup> Nelson A. M. Pereira,<sup>†</sup> João Dias-Ferreira,<sup>‡,⊥</sup> Marta Piñeiro,<sup>†</sup> Maria Filomena Botelho,<sup>‡,⊥</sup> and Teresa M. V. D. Pinho e Melo<sup>\*,†,⊥</sup>

<sup>†</sup>CQC and Department of Chemistry, University of Coimbra, 3004-535 Coimbra, Portugal

<sup>‡</sup>Biophysics Institute and Institute for Clinical and Biomedical Research (iCBB), area of Environment Genetics and Oncobiology (CIMAGO), Faculty of Medicine and <sup>⊥</sup>CNC.IBILI Consortium, University of Coimbra, 3004-548 Coimbra, Portugal

## Supporting Information

**ABSTRACT:** Ring-fused diphenylchlorins as potent low-dose photosensitizers for photodynamic therapy of bladder carcinoma and esophageal adenocarcinoma are described. All studied molecules were very active against HT1376 urinary bladder carcinoma and OE19 esophageal adenocarcinoma cell lines, showing IC<sub>50</sub> values below 50 nM. The in vivo evaluation of the more promising photosensitizer, using an OE19 tumor/chick embryo chorioallantoic membrane model, showed a tumor weight regression of 33% with a single photodynamic therapy treatment with the photosensitizer dose as low as 37 ng/embryo.



## 1. INTRODUCTION

Photodynamic therapy (PDT) has been used in the treatment of several types of cancers<sup>1–8</sup> and also in other diseases, such as actinic keratosis,<sup>9–11</sup> acne,<sup>12,13</sup> Barrett's esophagus,<sup>14,15</sup> and age-related macular degeneration (AMD).<sup>16,17</sup> PDT is based on the administration of a photosensitizer (PS), which selectively locates itself in the tumor cells followed by visible light irradiation. Suitable light exposure of the tumor region leads to the formation of cytotoxic reactive oxygen species (ROS), for example, hydroxyl radicals, the superoxide anion, and singlet oxygen, that induce cell death. These features provide PDT with an interesting and much valued dual selectivity.<sup>18</sup> Photosensitizer molecules should be activated with light of 600 to 800 nm wavelengths, the phototherapeutic window, which bears enough energy to produce ROS, can reach deeper into the tissues and avoid excitation of endogenous chromophores.<sup>19,20</sup> Therefore, one of the desirable characteristics of the photosensitizer is to absorb strongly within this range. In fact, the most efficient porphyrin-derived PSs are chlorins, hydroporphyrins that present typically intense absorption bands in the red and near-infrared (NIR) regions. Among these, either currently approved or in clinical trials, chlorins Foscan,<sup>22–25</sup> Verteporfin,<sup>26,27</sup> and Radachlorin<sup>28,29</sup> stand out.

The synthetic strategies for the preparation of chlorins have been centered on modifications of naturally occurring chlorins, total synthesis, and transformation of porphyrins via reduction, cycloaddition, and annulation reactions<sup>20,30–34</sup> with the most common one being based on Whitlock's method of porphyrin reduction with diimide.<sup>35</sup> However, this methodology affords

chlorins with limited stability due to the easy reoxidation to the porphyrin state and leads to the formation of by-products, for example, other hydroporphyrins, making the purification process extremely difficult in some cases. Our contribution overcame this with the development of a new class of highly stable ring-fused chlorins. Novel 4,5,6,7-tetrahydropyrazolo-[1,5-*a*]pyridine-fused chlorins were synthesized via [8 $\pi$  + 2 $\pi$ ] cycloaddition of transient 1,7-dipole diazafulvenium methides with porphyrins.<sup>36,37</sup> Further studies demonstrated that this kind of ring-fused *meso*-tetraphenylchlorins, particularly a new dihydroxymethyl derivative, has an impressive performance against human skin malignant melanoma.<sup>38</sup> Furthermore, the incorporation of the platinum(II) metal into their structure originated excellent theranostic agents for imaging, PDT, and molecular oxygen sensing.<sup>39</sup>

Our contribution to PDT of melanoma extended to the study of novel ring-fused 5,15-diphenylchlorins (Figure 1). These chlorins were even more photocytotoxic against A375 skin malignant melanoma cells than the corresponding tetraphenyl analogues, presenting IC<sub>50</sub> values as low as 2.9 nM.<sup>40</sup> Furthermore, for one of the derivatives (chlorin 3), the cell death outcome, apoptosis versus necrosis, was determined by its concentration. This can be explored to control the type of cell death in order to improve the effectiveness of PDT considering that an inflammatory response resulting from necrotic cell death after PDT can activate the antitumor

Received: June 22, 2019

Accepted: August 21, 2019

Published: October 9, 2019

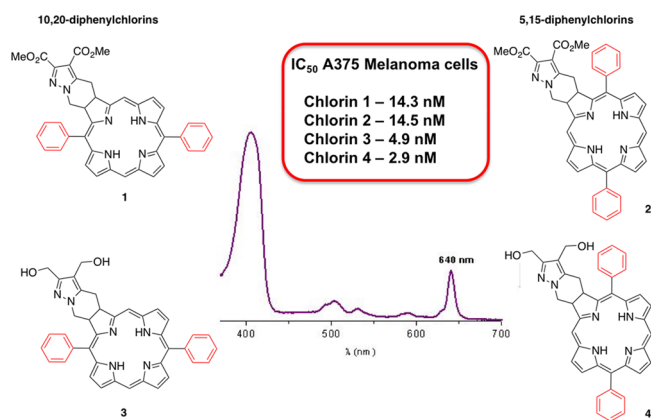


**Figure 1.** Chemical structures, UV-vis absorption spectra, and  $IC_{50}$  values against A375 melanoma cells of chlorins 1–4.<sup>40</sup>

immune response with implications also on vascular damage.<sup>20,21</sup> This feature combined with very low dark cytotoxicity makes chlorin 3 a particular interesting photosensitizer for PDT.

These outstanding results led us to further explore chlorins 1–4 as PDT agents against other selected cancers. PDT has been proven beneficial to both esophageal and urinary bladder carcinomas due to easy endoscopic irradiation, representing an effective, powerful, and minimally invasive treatment option.<sup>41,42</sup> The use of PDT in these tumors offered long survival periods and even a cure for some patients.<sup>43–46</sup> To take a step forward and further examine the photosensitizing capabilities of these ring-fused diphenylchlorins, we decided to spread the scope of our research by carrying out early *in vivo* assessment of the more promising photosensitizer using the chick embryo chorioallantoic membrane (CAM) model. Although the use of PSs and their accomplishments concerning vascular development and angiogenesis,<sup>47,48</sup> tissular  $O_2$  measuring,<sup>49,50</sup> and cancer diagnostics<sup>51,52</sup> have been reported using this model, this is still a somewhat underutilized *in vivo* assay when it comes to cancer PDT.<sup>53,54</sup> Details on our latest work regarding the aforementioned topics are herein disclosed.

## 2. RESULTS AND DISCUSSION

Ring-fused diphenylchlorins 1–4 were prepared and isolated following synthetic procedures established at our labs and previously described (Figure 1).<sup>37,40</sup> 5,15-Diphenylporphyrin was reacted with the diazafulvenium methide generated *in situ* from dimethyl 2,2-dioxo-1*H*,3*H*-pyrazolo[1,5-*c*][1,3]thiazole-6,7-dicarboxylate to afford the target 10,20-diphenylchlorins 1 and 2. The reduction of these diester chlorins (1 and 2) with lithium aluminum hydride led to the corresponding dihydroxymethyl chlorins (3 and 4).<sup>37,40</sup> Chlorins 1–4 present photophysical properties that are adequate to their use as photosensitizers with high absorption at the therapeutic window and moderate to high singlet oxygen quantum yields.

The photocytotoxicity of ring-fused diphenylchlorins 1–4 against human HT1376 urinary bladder carcinoma and OE19 esophageal adenocarcinoma cell lines was investigated; the corresponding dose–response curves are presented in Figure 2, and related  $IC_{50}/CI_{95}$  values are summarized in Table 1. PDT toxicity evaluation was carried out 24 h after irradiation (a fluence rate of 7.5 mW/cm<sup>2</sup>, total fluence of 10 J, and a filtered light source with a cutoff of <560 nm). Chlorins 1–4 showed high phototoxicity against bladder carcinoma cells with  $IC_{50}$

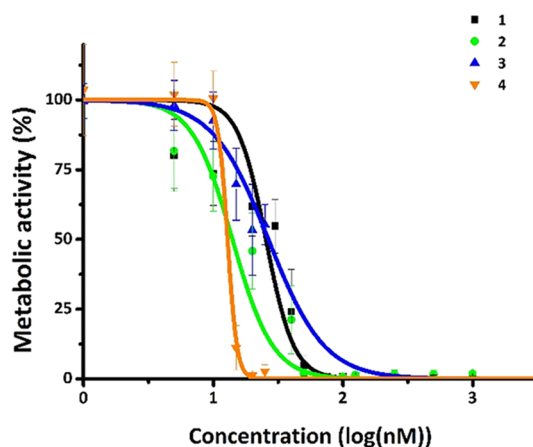
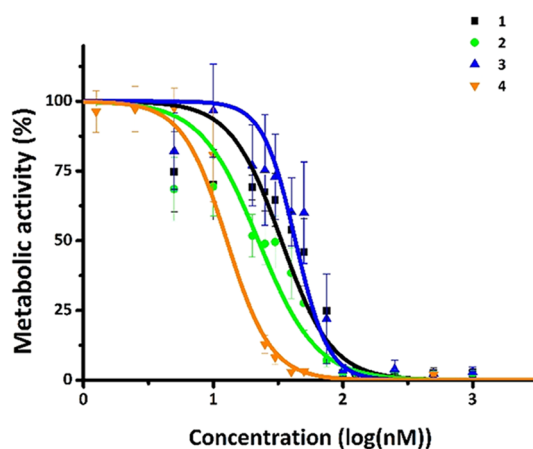


**Figure 2.** Dose–response curves of HT1376 (above) and OE19 (below). Analysis was performed 24 h after PDT using chlorins 1–4 with energy of 10 J. Data points represent the mean  $\pm$  SD.

**Table 1.**  $IC_{50}$  and Respective Confidence Intervals at 95% ( $CI_{95}$ ) of Chlorins 1–4 in HT1376 and OE19 Cells<sup>a</sup>

chlorin	photocytotoxicity (nM)			
	HT1376		OE19	
	$IC_{50}$	$CI_{95}$	$IC_{50}$	$CI_{95}$
1	33.6	[26.7; 42.3]	25.5	[20.5; 34.7]
2	22.3	[15.9; 31.4]	14.1	[8.4; 23.5]
3	43.0	[33.0; 56.1]	26.6	[20.5; 34.7]
4	12.8	[9.8; 16.6]	12.9	[11.1; 15.0]

<sup>a</sup>Analysis was performed 24 h after PDT with energy of 10 J. Values were determined by dose–response sigmoidal fitting.

values between 12.8 and 43.0 nM. Photocytotoxicity was also very high against esophageal adenocarcinoma cells with  $IC_{50}$  values below 26.6 nM. Therefore, chlorins 1–4 were demonstrated to be remarkably powerful low-dose photosensitizing agents showing  $IC_{50}$  values below 50 nM against all tumor cell lines studied.

5,15-Diphenylchlorins either with exocyclic methyl ester or hydroxymethyl functionalities, 2 and 4, respectively, proved to be better photodynamic agents against both cell lines than 10,20-diphenylchlorins 1 and 3. There was a curious change regarding the previously reported results on the PDT activity of diphenylchlorins 1–4 against melanoma (A375 cells) where the more hydrophilic hydroxymethyl chlorins 3 and 4 were approximately 3 to 5 times more active than their equivalent

methyl ester analogues **1** and **2**.<sup>40</sup> A different structure–activity trend was observed with HT1376 and OE19 cells. Hence, in addition to the overall hydrophilic/hydrophobic nature of the diphenylchlorin scaffold, it appears that the diphenyl substitution pattern of the macrocycle, 5,15-diphenylchlorins versus 10,20-diphenyl, is an important aspect and might play a differentiating part with regard to the photodynamic therapy efficiency of this type of photosensitizers across distinct tumor cells.

The chick embryo has long been used as a prototypical organism in several research areas, including oncobiology,<sup>55</sup> although studies on photodynamic therapy are scarce.<sup>53,54</sup> It is surrounded by the CAM, a highly vascularized extra-embryonic membrane that can effortlessly be used to graft human cells. When implanted on the CAM, tumor cells are capable of stimulating the formation of new blood vessels, gaining their blood supply, which in turn allows them to develop in a related fashion as in their natural hosts, that is, to proliferate, invade, and metastasize to the chick embryonic organs. This presents several key advantages over other standard animal models: the chick embryo is naturally immunodeficient, thus easily allowing mammalian tissue xenografts; the procedures are relatively simple, involving short experimental times and low costs. Also, regarding the protection of animals used for scientific purposes, the use of nonmammal embryos does not encompass any legal or ethical restrictions.<sup>55–57</sup>

In a previous study, we demonstrated that chlorins **3** and **4** show a melanoma A375 cell uptake significantly higher than the ones observed for the corresponding diester derivatives **1** and **2**.<sup>40</sup> On the other hand, *in vitro* data showed some decrease in the metabolic activity of both A375 skin malignant melanoma and HFF-1 fibroblast cells after exposure to chlorin **4**. Thus, dihydroxymethyl chlorin **3** showing no dark *in vitro* cytotoxicity was selected for the *in vivo* chick embryo CAM assessment of a human OE19 esophageal adenocarcinoma model. The schematic protocol and timeline for this study is presented in Figure 3.

After nine days of incubation (E9), when the embryo has reached adequate development, the chorioallantoic membrane of White Leghorn chicken eggs was grafted with OE19 cells. At day 11 (E11), all groups of eggs were treated with either the administration vehicle (1% DMSO in PBS, groups I and III) or

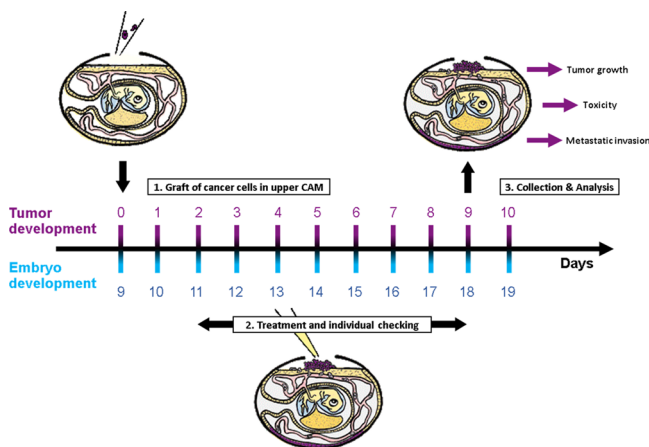


**Figure 3.** Schematic illustration and timeline for the *in vivo* chick embryo CAM assay (replicated with permission from Inovotion SAS, La Tronche/Grenoble, France).

chlorin **3** (608 nM, groups II and IV). Ten minutes after administration, eggs of groups III and IV were subjected to light irradiation using the conditions indicated in the Supporting Information (see Table S1).

The number of dead and alive chick embryos was fully counted at E18 and combined with the surveillance of visible and macroscopic anomalies (see Table S2); the key data are displayed in Figure 4. Interestingly, we observed an ~50%

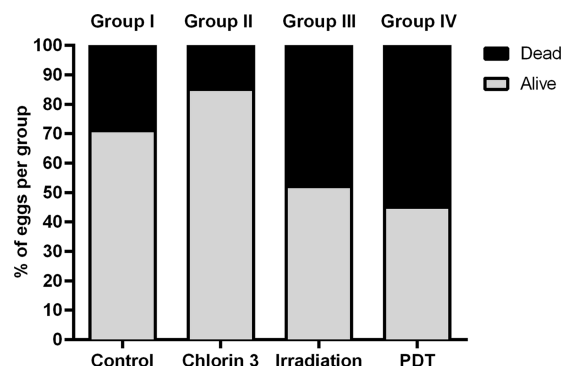


**Figure 4.** *In vivo* chick embryo CAM assay toxicity analysis, presenting the total, alive, and dead chick embryos for each group of eggs after treatment at E18.

chick embryo mortality rate in both light-exposed groups III and IV, but none whatsoever when only chlorin **3** was administered in group II (15% compared to 29% in the control group). This is a highly relevant outcome of the toxicity assay performed because it markedly demonstrates that the chick embryo mortality attained in the PDT group is mainly due to the illumination conditions applied.

At day 18 (E18) of the *in vivo* chick embryo CAM assay, the CAM was collected and analyzed (see Figure 3). As can be seen in Table S3 and Figure 5, no substantial tumor weight variation compared to the control group was observed in groups II and III, which means that neither ring-fused chlorin **3** nor light irradiation per se produced a cytotoxic outcome on OE19 cells. However, the combination of the two, group IV,

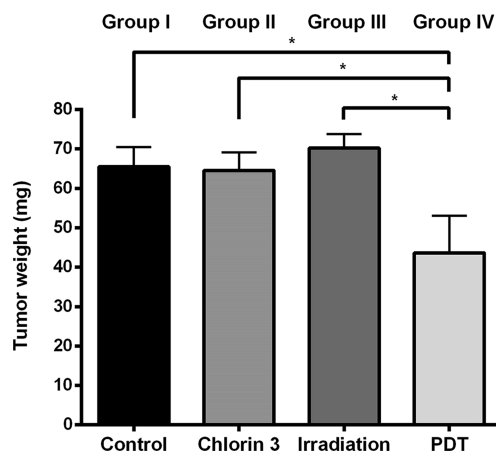


**Figure 5.** *In vivo* chick embryo CAM assay tumor growth analysis, presenting mean values  $\pm$  SEM of tumor weights (mg) for each group of eggs after treatment. The upper portion of the CAM was detached at E18, and the tumors were carefully removed from normal tissue and weighed. Significant differences are represented by \* where \* means  $p < 0.05$ .

that is, the PDT treatment group, prompted a substantial photodynamic effect with a tumor weight regression of 33% reached with a single-treatment protocol with the photosensitizer dose as low as 37 ng/embryo.

Genomic DNA was extracted from the CAM and analyzed by quantitative polymerase chain reaction (qPCR) with specific primers for Alu sequences. Since these are primate-specific short interspersed elements (SINEs) with over 1 million copies of which are present in the human genome, Alu sequences are useful targets for detecting human cells.<sup>58,59</sup> From the information exhibited in Figure 6, it was possible to

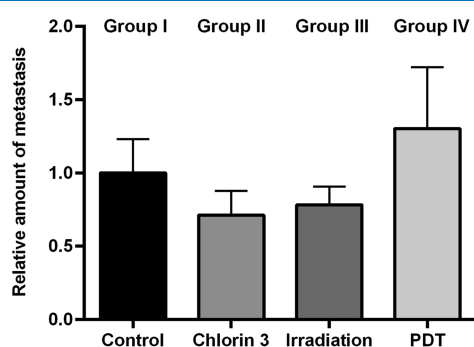


**Figure 6.** In vivo chick embryo CAM assay metastasis invasion analysis, presenting relative amounts of metastasis in the lower CAM for each group of eggs after treatment compared to the control group (in which an arbitrary value of 1 was chosen). The effect on the metastatic invasion of the OE19 cells was evaluated in a portion of the lower CAM collected at E18. No significant differences were found between groups.

infer that no consequence, either beneficial or detrimental, was verified in any of the treatment groups under scrutiny, that is, the application of chlorin 3 or light irradiation on its own and the PDT group, given that the fold variation of the relative amount of metastasis (RQ value) compared to the control group/calibrator (which was arbitrarily set to 1) was only  $\pm 0.3$  at the most. This value is less than the 2-fold change (RQ value greater than 2 or minor than 0.5) typically required to be considered significant.<sup>60,61</sup> Regarding the mean cycle quantification (mean Cq) values attained, it stands to reason that the number of cycles needed for a fluorescence signal to be detected was quite nearly the same in all samples studied, between 25.41 and 26.28, regardless of the treatment groups and conditions (see Table S4). Therefore, our study demonstrated that a nanomolar dose is enough to observe a PDT effect in the tumor at the upper CAM without an antimetastatic effect in the lower CAM.

### 3. CONCLUSIONS

In conclusion, the photocytotoxicity of 4,5,6,7-tetrahydropyrazolo[1,5-*a*]pyridine-fused 10,20-diphenylchlorins and 5,15-diphenylchlorins against human HT1376 urinary bladder carcinoma and OE19 esophageal adenocarcinoma cell lines was examined, and  $IC_{50}$  values of 12.8–43.0 and 12.9–26.6 nM, respectively, were obtained. All molecules proved to be extraordinarily potent low-dose PSs.

Furthermore, structure–activity relationships could be identified. The diphenyl substitution pattern of the macrocycle, 5,15-diphenylchlorins versus 10,20-diphenyl, is the structural feature with higher impact on the modulation of the PDT activity, although the overall hydrophilicity/hydrophobicity of

the diphenylchlorin scaffold must also be considered. In fact, the diester as well as the dihydroxymethyl 5,15-diphenylchlorin derivatives presented a slightly superior photodynamic action against both cell lines to their corresponding isomeric 10,20-diphenylchlorins.

Dihydroxymethyl 5,15-diphenylchlorin was chosen for the in vivo evaluation using an OE19 tumor/chick embryo CAM model. Despite their high photodynamic activity, this photosensitizer did not show cytotoxicity per se since the chick embryo survival rate was very high (85%) when the chlorin was applied without photoactivation. On the other hand, no significant tumor weight variation was observed when the chlorin or light irradiation was employed per se. Therefore, it was only under the photodynamic treatment conditions that phototoxicity was observed leading to a considerable tumor weight regression of 33% in a single-PDT treatment while using a very low dose in the range of tens of nanograms per embryo.

### 4. EXPERIMENTAL SECTION

Chlorins were prepared from the reaction of 2,2-dioxo-1*H*,3*H*-pyrazolo[1,5-*c*][1,3]thiazole-6,7-dicarboxylate and 5,15-diphenylporphyrin under microwave irradiation as previously described.<sup>39</sup>

**4.1. In Vitro Tumor Cell Biology Assay.** **4.1.1. Cell Culture Conditions.** The human HT1376 (CRL1472) urinary bladder carcinoma cell line was purchased from the American Type Culture Collection. The human OE19 (96071721) esophageal adenocarcinoma cell line was purchased from the European Collection of Authenticated Cell Cultures. The cell lines were cultured according to standard procedures at 37 °C in a humidified incubator with 95% air and 5% CO<sub>2</sub>. HT1376 cells were expanded using the Dulbecco's Modified Eagle Medium (DMEM, Sigma D-5648), supplemented with 10% heat-inactivated fetal bovine serum (FBS, Sigma F7524), 1% penicillin–streptomycin (100 U/mL penicillin and 10 mg/mL streptomycin, Gibco 15140-122), and 100  $\mu$ M sodium pyruvate (Gibco Invitrogen Life Technologies; Gibco 1360). OE19 cells were expanded using the Roswell Park Memorial Institute 1640 medium (RPMI 1640, Sigma R4130), supplemented with 10% heat-inactivated fetal bovine serum (FBS, Sigma F7524), 1% penicillin–streptomycin (100 U/mL penicillin and 10 mg/mL streptomycin, Gibco 15140-122), and 400 mM sodium pyruvate (Gibco Invitrogen Life Technologies; Gibco 1360). For all studies, cells were detached using a solution of 0.25% trypsin–EDTA (Gibco).

**4.1.2. Photodynamic Treatment.** For each experiment, cells were plated and kept in an incubator overnight to allow the attachment of the cells. The formulation of the chlorin photosensitizers consisted of a 1 mg/mL solution in DMSO (Fisher Chemical, 200-664-3) with the desired concentrations achieved by successive dilutions. Photosensitizers were administered in several concentrations (from 5 pM to 10  $\mu$ M), and cells were incubated for 24 h. Controls were included on every plate, including untreated cell cultures and cultures treated only with the vehicle of administration of the photosensitizers. For this, DMSO was always administered with a concentration of 1%. Cells were washed with phosphate buffered saline (PBS; in mM: 137 NaCl (JMGs), 2.7 KCl (Sigma), 10 Na<sub>2</sub>HPO<sub>4</sub> (Merck), and 1.8 KH<sub>2</sub>PO<sub>4</sub> (Sigma); pH 7.4), and a new drug-free medium was added. Each plate was irradiated with a fluence rate of 7.5 mW/cm<sup>2</sup> until a total of 10 J was reached using a light source equipped with a red filter

(cutoff of <560 nm). Evaluation was performed 24 h after photodynamic treatment.

**4.1.3. Photocytotoxicity Analysis.** The sensitivity of the cell lines to the chlorin photosensitizers was analyzed using the MTT colorimetric assay (Sigma M2128; Sigma-Aldrich, Inc.) to measure metabolic activity. Cell culture plates were washed and incubated with a solution of 3-(4,5-dimethylthiazol-2-yl)-2,5-diphenyltetrazolium bromide (0.5 mg/mL, Sigma M5655) in PBS, pH 7.4, in the dark at 37 °C for at least 4 h. To solubilize formazan crystals, a 0.04 M solution of hydrochloric acid (Merck Millipore 100317) in isopropanol (Sigma 278475) was added. Absorbance was measured using an EnSpire Multimode Plate Reader (Perkin Elmer). Photocytotoxicity was expressed as the percentage relative to cell cultures treated only with the vehicle of administration of the photosensitizers. Dose–response curves were obtained using Origin 9.0, and the concentration of the photosensitizers that inhibits the proliferation of cultures at 50% (IC<sub>50</sub>) was derived.

**4.2. In Vivo Chick Embryo CAM Assay.** **4.2.1. Materials.** Fertilized White Leghorn chicken eggs (Hendrix Genetics, Saint Brieu, France) were incubated at 37.5 °C with 50% relative humidity for nine days. At this time (E9), the chorioallantoic membrane (CAM) was dropped down by carefully drilling a small hole through the eggshell into the air sac, and a 1 cm<sup>2</sup> window was cut in the eggshell directly above the CAM.

**4.2.2. Tumor Cell Induction.** Human OE19 esophageal adenocarcinoma cells were cultured and expanded as described above, harvested by trypsinization, washed with complete medium, and suspended in a serum-free graft medium. An inoculation of 5 × 10<sup>5</sup> cells onto the CAM of each egg was made at day 9 (E9). The eggs were then randomly allocated into 4 groups with at least 20 eggs/group.

**4.2.3. Treatment.** At day 10 (E10), tumors began to be detectable. At day 11 (E11), the groups were treated with 100 μL of chlorin 3 (608 nM) or the administration vehicle (1% DMSO in PBS), following the conditions summarized in the Supporting Information (see Table S1). Ten minutes after injection in the tumor mass, eggs of groups III and IV were placed under the light source (a CoolLED pE-4000 universal illumination system equipped with a collimator, see Figure S1) for irradiation using red light (635 nm) with a fluence of 2.5 J/cm<sup>2</sup>. The light source with a collimator was previously calibrated on eggs grafted with OE19 cells at day 11 (E11) using white light in order to achieve efficient illumination closely around the treated area, that is, centered on the tumor (see Figure S2, top). The distance between the surface of the upper CAM and the light source with the collimator was 26 cm, and the diameter of the circle illuminated in the upper CAM was 2.5 cm (see Figure S2, bottom). The time of irradiation needed to reach 2.5 J/cm<sup>2</sup> was 1 min at 83 mW.

**4.2.4. Tumor Growth Analysis.** At day 18 (E18), the upper portion of the CAM was removed, washed with PBS and then directly transferred in 4% *p*-formaldehyde solution (fixation for 48 h). The tumors were then carefully cut away from normal CAM tissue and weighed. A one-way ANOVA analysis with post-hoc tests was then performed on the data (see Table S3).

**4.2.5. Metastasis Invasion Analysis.** A 1 cm<sup>2</sup> portion of the lower CAM was collected to evaluate the number of metastasis cells. Genomic DNA was extracted from the CAM using a commercial kit (MagJET Genomic DNA Kit, Ref. K2721, Thermo Scientific) and analyzed by quantitative polymerase chain reaction (qPCR) with specific primers for human Alu

sequences (sense: 5'-ACG CCT GTA ATC CCA GCA CTT-3'; antisense: 5'-TCG CCC AGG CTG GAG TGCA-3'). The amplification and detection of these Alu sequences by qPCR was performed on 30 ng of genomic DNA in a final volume of 20 μL/point using a Bio-Rad CFX96 Touch detection system with the following conditions: 95 °C for 2 min followed by 35 cycles at 95 °C for 30 s, 63 °C for 30 s, and 72 °C for 30 s. The variation in the Alu signal relative to the total amount of genomic DNA (and, therefore, changes in the quantity of human DNA in the CAM tissue) as well as statistical analysis on the data obtained was calculated using Bio-Rad CFX Maestro software (see Table S4).

**4.2.6. Toxicity Analysis.** The number of dead and alive chick embryos was totally counted seven days after treatment (E18) and combined with the observation of visible and macroscopic abnormalities (see Table S2).

## ■ ASSOCIATED CONTENT

### 📄 Supporting Information

The Supporting Information is available free of charge on the ACS Publications website at DOI: 10.1021/acsomega.9b01865.

Experimental section, in vitro tumor cell biology assay, data and setup of the in vivo chick embryo CAM assay (PDF)

## ■ AUTHOR INFORMATION

### Corresponding Author

\*E-mail: [tmelo@ci.uc.pt](mailto:tmelo@ci.uc.pt).

### ORCID

João Dias-Ferreira: 0000-0002-8502-8701

Maria Filomena Botelho: 0000-0001-7202-1650

Teresa M. V. D. Pinho e Melo: 0000-0003-3256-4954

### Author Contributions

All authors have given approval to the final version of the manuscript.

### Notes

The authors declare no competing financial interest.

## ■ ACKNOWLEDGMENTS

This work was funded by the Portuguese Foundation for Science and Technology (FCT) and co-funded by FEDER through COMPETE 2020 (project no. POCI-01-0145-FEDER-PTDC/QEQ-MED/0262/2014) and PT 2020/CENTRO 2020 (project no. CENTRO-01-0145-FEDER-000014/MATIS) and CIMAGO. The CQC is supported via project no. POCI-01-0145-FEDER-007630. The CNC.IBILI Consortium is supported by nos. PEst-UID/NEU/04539/2013 and POCI-01-0145-FEDER-007440.

## ■ REFERENCES

- (1) Van Straten, D.; Mashayekhi, V.; De Bruijn, H.; Oliveira, S.; Robinson, D. Oncologic photodynamic therapy: basic principles, current clinical status and future directions. *Cancers* **2017**, *9*, 19.
- (2) Dąbrowski, J. M.; Arnaut, L. G. Photodynamic therapy (PDT) of cancer: from local to systemic treatment. *Photochem. Photobiol. Sci.* **2015**, *14*, 1765–1780.
- (3) Ethirajan, M.; Chen, Y.; Joshi, P.; Pandey, R. K. The role of porphyrin chemistry in tumor imaging and photodynamic therapy. *Chem. Soc. Rev.* **2011**, *40*, 340–362.

- (4) Allison, R. R.; Sibata, C. H. Oncologic photodynamic therapy photosensitizers: A clinical review. *Photodiagn. Photodyn. Ther.* **2010**, *7*, 61–75.
- (5) O'Connor, A. E.; Gallagher, W. M.; Byrne, A. T. Porphyrin and nonporphyrin photosensitizers in oncology: Preclinical and clinical advances in photodynamic therapy. *Photochem. Photobiol.* **2009**, *85*, 1053–1074.
- (6) Triesscheijn, M.; Baas, P.; Schellens, J. H. M.; Stewart, F. A. Photodynamic therapy in oncology. *Oncologist* **2006**, *11*, 1034–1044.
- (7) Brown, S. B.; Brown, E. A.; Walker, I. The present and future role of photodynamic therapy in cancer treatment. *Lancet Oncol.* **2004**, *5*, 497–508.
- (8) Agostinis, P.; Berg, K.; Cengel, K. A.; Foster, T. H.; Girotti, A. W.; Gollnick, S. O.; Hahn, S. M.; Hamblin, M. R.; Juzeniene, A.; Kessel, D.; Korbelik, M.; Moan, J.; Mroz, P.; Nowis, D.; Piette, J.; Wilson, B. C.; Golab, J. Photodynamic therapy of cancer: An update. *Ca-Cancer J. Clin.* **2011**, *61*, 250–281.
- (9) de Oliveira, E. C. V.; da Motta, V. R. V.; Pantoja, P. C.; Ilha, C. S. d. O.; Magalhães, R. F.; Galadari, H.; Leonardi, G. R. Actinic keratosis – review for clinical practice. *Int. J. Dermatol.* **2019**, *58*, 400–407.
- (10) Ericson, M. B.; Wennberg, A.-M.; Larkö, O. Review of photodynamic therapy in actinic keratosis and basal cell carcinoma. *Ther. Clin. Risk Manage.* **2008**, *4*, 1–9.
- (11) Wlodek, C.; Ali, F. R.; Lear, J. T. Use of photodynamic therapy for treatment of actinic keratoses in organ transplant recipients. *BioMed Res. Int.* **2013**, *2013*, 349526.
- (12) Boen, M.; Brownell, J.; Patel, P.; Tsoukas, M. M. The role of photodynamic therapy in acne: An evidence-based review. *Am. J. Clin. Dermatol.* **2017**, *18*, 311–321.
- (13) Keyal, U.; Bhatta, A. K.; Wang, X. L. Photodynamic therapy for the treatment of different severity of acne: A systematic review. *Photodiagn. Photodyn. Ther.* **2016**, *14*, 191–199.
- (14) Kelty, C. J.; Marcus, S. L.; Ackroyd, R. Photodynamic therapy for Barrett's esophagus: a review. *Dis. Esophagus* **2002**, *15*, 137–144.
- (15) Qumseya, B. J.; David, W.; Wolfsen, H. C. Photodynamic therapy for Barrett's esophagus and esophageal carcinoma. *Clin. Endosc.* **2013**, *46*, 30–37.
- (16) Wormald, R.; Evans, J. R.; Smeeth, L. L.; Henshaw, K. S. Photodynamic therapy for neovascular age-related macular degeneration. *Cochrane Database Syst. Rev.* **2007**, DOI: [10.1002/14651858.CD002030.pub2](https://doi.org/10.1002/14651858.CD002030.pub2).
- (17) Wormald, R.; Evans, J. R.; Smeeth, L. L.; Henshaw, K. S. Photodynamic therapy for neovascular age-related macular degeneration. *Cochrane Database Syst. Rev.* **2005**, DOI: [10.1002/14651858.CD002030.pub2](https://doi.org/10.1002/14651858.CD002030.pub2).
- (18) Castano, A. P.; Demidova, T. N.; Hamblin, M. R. Mechanisms in photodynamic therapy: part one-photosensitizers, photochemistry and cellular localization. *Photodiagn. Photodyn. Ther.* **2004**, *1*, 279–293.
- (19) Plaetzer, K.; Krammer, B.; Berlanda, J.; Berr, F.; Kiesslich, T. Photophysics and photochemistry of photodynamic therapy: fundamental aspects. *Lasers Med. Sci.* **2009**, *24*, 259–268.
- (20) Abrahamse, H.; Hamblin, M. R. New photosensitizers for photodynamic therapy. *Biochem. J.* **2016**, *473*, 347–364.
- (21) Tanaka, M.; Kataoka, H.; Yano, S.; Sawada, T.; Akashi, H.; Inoue, M.; Suzuki, S.; Inagaki, Y.; Hayashi, N.; Nishie, H.; Shimura, T.; Mizoshita, T.; Mori, Y.; Kubota, E.; Tanida, S.; Takahashi, S.; Joh, T. Immunogenic cell death due to a new photodynamic therapy (PDT) with glycoconjugated chlorin (G-chlorin). *Oncotarget* **2016**, *7*, 47242–47251.
- (22) Dilkes, M. G.; DeJode, M. L.; Rowntree-Taylor, A.; McGilligan, J. A.; Kenyon, G. S.; McKelvie, P. m-THPC photodynamic therapy for head and neck cancer. *Lasers Med. Sci.* **1996**, *11*, 23–29.
- (23) Kübler, A. C.; de Carpentier, J.; Hopper, C.; Leonard, A. G.; Putnam, G. Treatment of squamous cell carcinoma of the lip using Foscan-mediated Photodynamic Therapy. *Int. J. Oral Surg.* **2001**, *30*, 504–509.
- (24) Copper, M. P.; Tan, I. B.; Oppelaar, H.; Ruevekamp, M. C.; Stewart, F. A. Meta-tetra(hydroxyphenyl)chlorin photodynamic therapy in early-stage squamous cell carcinoma of the head and neck. *Arch. Otolaryngol., Head Neck Surg.* **2003**, *129*, 709–711.
- (25) Hopper, C.; Kübler, A.; Lewis, H.; Tan, I. B.; Putnam, G.; the Foscan 01 Study Group. mTHPC-mediated photodynamic therapy for early oral squamous cell carcinoma. *Int. J. Cancer* **2004**, *111*, 138–146.
- (26) Huggett, M. T.; Jermyn, M.; Gillams, A.; Illing, R.; Mosse, S.; Novelli, M.; Kent, E.; Bown, S. G.; Hasan, T.; Pogue, B. W.; Pereira, S. P. Phase I/II study of verteporfin photodynamic therapy in locally advanced pancreatic cancer. *Br. J. Cancer* **2014**, *110*, 1698–1704.
- (27) Isakoff, S. J.; Rogers, G. S.; Hill, S.; McMullan, P.; Habin, K. R.; Park, H.; Bartenstein, D. W.; Chen, S. T.; Barry, W. T.; Overmoyer, B. An open label, phase II trial of continuous low-irradiance photodynamic therapy (CLIPT) using verteporfin for the treatment of cutaneous breast cancer metastases. *J. Clin. Oncol.* **2017**, *35*, TPS1121.
- (28) Ji, W.; Yoo, J.-w.; Bae, E. K.; Lee, J. H.; Choi, C.-M. The effect of Radachlorin® PDT in advanced NSCLC: A pilot study. *Photodiagn. Photodyn. Ther.* **2013**, *10*, 120–126.
- (29) Kochneva, E. V.; Filonenko, E. V.; Vakulovskaya, E. G.; Scherbakova, E. G.; Seliverstov, O. V.; Markichev, N. A.; Reshetnikov, A. V. Photosensitizer Radachlorin® : Skin cancer PDT phase II clinical trials. *Photodiagn. Photodyn. Ther.* **2010**, *7*, 258–267.
- (30) Dudkin, S. V.; Makarova, E. A.; Lukyanets, E. A. Synthesis of chlorins, bacteriochlorins and their tetraaza analogues. *Russ. Chem. Rev.* **2016**, *85*, 700–730.
- (31) Taniguchi, M.; Lindsey, J. S. Synthetic Chlorins, Possible surrogates for chlorophylls, prepared by derivatization of porphyrins. *Chem. Rev.* **2016**, *117*, 344–535.
- (32) Pineiro, M.; Serra, A. C.; Pinho e Melo, T. M. V. D., Synthetic strategies to chlorins and bacteriochlorins. In *Handbook of Porphyrins: Chemistry, Properties and Applications*, Kaibara, A.; Matsumura, G. Ed.; Nova Science Publishers, Inc.: USA, 2012, pp 89–160.
- (33) Zhang, J.; Jiang, C.; Figueiró Longo, J. P.; Azevedo, R. B.; Zhang, H.; Muehlmann, L. A. An updated overview on the development of new photosensitizers for anticancer photodynamic therapy. *Acta Pharm. Sin. B* **2018**, *8*, 137–146.
- (34) Chen, H.; Humble, S. W.; Jinadasa, R. G. W.; Zhou, Z.; Nguyen, A. L.; Vicente, M. G. H.; Smith, K. M. Syntheses and PDT activity of new mono- and di-conjugated derivatives of chlorin e6. *J. Porphyrins Phthalocyanines* **2017**, *21*, 354–363.
- (35) Whitlock, H. W.; Hanauer, R.; Oester, M. Y.; Bower, B. K. Diimide reduction of porphyrins. *J. Am. Chem. Soc.* **1969**, *91*, 7485–7489.
- (36) Pereira, N. A. M.; Serra, A. C.; Pinho e Melo, T. M. V. D. Novel approach to chlorins and bacteriochlorins:  $[8\pi+2\pi]$  Cycloaddition of diazafulvenium methides with porphyrins. *Eur. J. Org. Chem.* **2010**, 6539–6543.
- (37) Pereira, N. A. M.; Fonseca, S. M.; Serra, A. C.; Pinho e Melo, T. M. V. D.; Burrows, H. D.  $[8\pi+2\pi]$  Cycloaddition of meso-tetra- and 5,15-diarylporphyrins: Synthesis and photophysical characterization of stable chlorins and bacteriochlorins. *Eur. J. Org. Chem.* **2011**, 3970–3979.
- (38) Pereira, N. A. M.; Laranjo, M.; Pineiro, M.; Serra, A. C.; Santos, K.; Teixo, R.; Abrantes, A. M.; Gonçalves, A. C.; Sarmiento Ribeiro, A. B.; Casalta-Lopes, J.; Botelho, M. F.; Pinho e Melo, T. M. V. D. Novel 4,5,6,7-tetrahydropyrazolo[1,5-a]pyridine fused chlorins as very active photodynamic agents for melanoma cells. *Eur. J. Med. Chem.* **2015**, *103*, 374–380.
- (39) Pereira, N. A. M.; Laranjo, M.; Casalta-Lopes, J.; Serra, A. C.; Piñeiro, M.; Pina, J.; Seixas de Melo, J. S.; Senge, M. O.; Botelho, M. F.; Martelo, L.; Burrows, H. D.; Pinho e Melo, T. M. V. D. Platinum(II) ring-fused chlorins as near-infrared emitting oxygen sensors and photodynamic agents. *ACS Med. Chem. Lett.* **2017**, *8*, 310–315.
- (40) Pereira, N. A. M.; Laranjo, M.; Pina, J.; Oliveira, A. S. R.; Ferreira, J. D.; Sánchez-Sánchez, C.; Casalta-Lopes, J.; Gonçalves, A.

- C.; Sarmiento-Ribeiro, A. B.; Piñeiro, M.; Seixas de Melo, J. S.; Botelho, M. F.; Pinho e Melo, T. M. V. D. Advances on photodynamic therapy of melanoma through novel ring-fused 5,15-diphenylchlorins. *Eur. J. Med. Chem.* **2018**, *146*, 395–408.
- (41) Raikar, R.; Agarwal, P. K. Photodynamic therapy in the treatment of bladder cancer: Past challenges and current innovations. *Eur. Urol. Focus* **2018**, *4*, 509–511.
- (42) Wu, H.; Minamide, T.; Yano, T. Role of photodynamic therapy in the treatment of esophageal cancer. *Dig. Endosc.* **2019**, DOI: 10.1111/den.13353.
- (43) Sibille, A.; Lambert, R.; Souquet, J. C.; Sabben, G.; Descos, F. Long-term survival after photodynamic therapy for esophageal cancer. *Gastroenterology* **1995**, *108*, 337–344.
- (44) Lindenmann, J.; Matzi, V.; Neuboeck, N.; Anegg, U.; Baumgartner, E.; Maier, A.; Smolle, J.; Smolle-Juettner, F. M. Individualized, multimodal palliative treatment of inoperable esophageal cancer: Clinical impact of photodynamic therapy resulting in prolonged survival. *Lasers Surg. Med.* **2012**, *44*, 189–198.
- (45) Nseyo, U. O.; DeHaven, J.; Dougherty, T. J.; Potter, W. R.; Merrill, D. L.; Lundahl, S. L.; Lamm, D. L. Photodynamic therapy (PDT) in the treatment of patients with resistant superficial bladder cancer: A long term experience. *Photomed. Laser Surg.* **1998**, *16*, 61–68.
- (46) Bader, M. J.; Stepp, H.; Beyer, W.; Pongratz, T.; Sroka, R.; Kriegmair, M.; Zaak, D.; Welschhof, M.; Tilki, D.; Stief, C. G.; Waidelich, R. Photodynamic therapy of bladder cancer – A phase I study using hexaminolevulinate (HAL). *Urol. Oncol.: Semin. Orig. Invest.* **2013**, *31*, 1178–1183.
- (47) Weiss, A.; van den Bergh, H.; Griffioen, A. W.; Nowak-Sliwinska, P. Angiogenesis inhibition for the improvement of photodynamic therapy: The revival of a promising idea. *Biochim. Biophys. Acta, Rev. Cancer* **2012**, *1826*, 53–70.
- (48) Debefve, E.; Pegaz, B.; van den Bergh, H.; Wagnières, G.; Lange, N.; Ballini, J. P. Video monitoring of neovessel occlusion induced by photodynamic therapy with verteporfin (Visudyne®), in the CAM model. *Angiogenesis* **2008**, *11*, 235–243.
- (49) Huntosova, V.; Gay, S.; Nowak-Sliwinska, P. M.; Rajendran, S. K.; Zellweger, M.; van den Bergh, H.; Wagnières, G. In vivo measurement of tissue oxygenation by time-resolved luminescence spectroscopy: advantageous properties of dichlorotris(1, 10-phenanthroline)-ruthenium(II) hydrate. *J. Biomed. Opt.* **2014**, 077004.
- (50) Piffaretti, F. M.; Novello, A. M.; Kumar, R. S.; Forte, E.; Paulou, C.; Nowak-Sliwinska, P. M.; van den Bergh, H. E.; Wagnières, G. A. Real-time, in vivo measurement of tissular pO<sub>2</sub> through the delayed fluorescence of endogenous protoporphyrin IX during photodynamic therapy. *J. Biomed. Opt.* **2012**, 115007.
- (51) Mondon, K.; Zeisser-Labouèbe, M.; Gurny, R.; Möller, M. MPEG-hexPLA micelles as novel carriers for hypericin, a fluorescent marker for use in cancer diagnostics. *Photochem. Photobiol.* **2011**, *87*, 399–407.
- (52) Saw, C. L. L.; Olivo, M.; Chin, W. W. L.; Soo, K. C.; Heng, P. W. S. Superiority of N-methyl pyrrolidone over albumin with hypericin for fluorescence diagnosis of human bladder cancer cells implanted in the chick chorioallantoic membrane model. *J. Photochem. Photobiol., B* **2007**, *86*, 207–218.
- (53) Weiss, A.; Bonvin, D.; Berndsen, R. H.; Scherrer, E.; Wong, T. J.; Dyson, P. J.; Griffioen, A. W.; Nowak-Sliwinska, P. Angiostatic treatment prior to chemo- or photodynamic therapy improves anti-tumor efficacy. *Sci. Rep.* **2015**, 8990.
- (54) Weiss, A.; van Beijnum, J. R.; Bonvin, D.; Jichlinski, P.; Dyson, P. J.; Griffioen, A. W.; Nowak-Sliwinska, P. Low-dose angiostatic tyrosine kinase inhibitors improve photodynamic therapy for cancer: lack of vascular normalization. *J. Cell. Mol. Med.* **2014**, *18*, 480–491.
- (55) Ribatti, D. The chick embryo chorioallantoic membrane as a model for tumor biology. *Exp. Cell Res.* **2014**, *328*, 314–324.
- (56) Nowak-Sliwinska, P.; Segura, T.; Iruela-Arispe, M. L. The chicken chorioallantoic membrane model in biology, medicine and bioengineering. *Angiogenesis* **2014**, *17*, 779–804.
- (57) Kue, C. S.; Tan, K. Y.; Lam, M. L.; Lee, H. B. Chick embryo chorioallantoic membrane (CAM): an alternative predictive model in acute toxicological studies for anti-cancer drugs. *Exp. Anim.* **2015**, *64*, 129–138.
- (58) Walker, J. A.; Kilroy, G. E.; Xing, J.; Shewale, J.; Sinha, S. K.; Batzer, M. A. Human DNA quantitation using Alu element-based polymerase chain reaction. *Anal. Biochem.* **2003**, *315*, 122–128.
- (59) Zijlstra, A.; Mellor, R.; Panzarella, G.; Aimes, R. T.; Hooper, J. D.; Marchenko, N. D.; Quigley, J. P. A Quantitative analysis of rate-limiting steps in the metastatic cascade using human-specific real-time polymerase chain reaction. *Cancer Res.* **2002**, *62*, 7083–7092.
- (60) Schmittgen, T. D.; Livak, K. J. Analyzing real-time PCR data by the comparative C(T) method. *Nat. Protoc.* **2008**, *3*, 1101–1108.
- (61) Ginzinger, D. G. Gene quantification using real-time quantitative PCR: an emerging technology hits the mainstream. *Exp. Hematol.* **2002**, *30*, 503–512.